

The interstellar N₂ abundance towards HD 124314 from far-ultraviolet observations

David C. Knauth, B-G Andersson, Stephan R. McCandliss & H. Warren Moos

Department of Physics and Astronomy, The Johns Hopkins University, 3400 North Charles Street, Baltimore, Maryland 21218, USA

The abundance of interstellar molecular nitrogen (N₂) is of considerable importance: models of steady-state gas-phase interstellar chemistry^{1,2}, together with millimetre-wavelength observations^{3,4} of interstellar N₂H⁺ in dense molecular clouds predict that N₂ should be the most abundant nitrogen-bearing molecule in the interstellar medium. Previous attempts to detect N₂ absorption in the far-ultraviolet⁵ or infrared⁶ (ice features) have hitherto been unsuccessful. Here we report the detection of interstellar N₂ at far-ultraviolet wavelengths towards the moderately reddened star HD 124314 in the constellation of Centaurus. The N₂ column density is larger than expected from models of diffuse clouds and significantly smaller than expected for dense molecular clouds¹. Moreover, the N₂ abundance does not explain the observed variations⁷ in the abundance of atomic nitrogen (N I) towards high-column-density sightlines, implying that the models of nitrogen chemistry in the interstellar medium are incomplete⁸.

Although N₂ was unsuccessfully searched for with the Copernicus satellite⁵, the Far Ultraviolet Spectroscopic Explorer (FUSE) enables sensitive probes of sightlines with large amounts of interstellar extinction. Archival observations of HD 124314 were acquired on 22 March 2000 using the large aperture (30" × 30") in the histogram data collection mode. HD 124314 is an O6Vnf star⁹ with visual magnitude *V* = 6.64 mag (ref. 10) and a moderate amount of interstellar reddening (*E*(*B*−*V*) = 0.53; ref. 11) equivalent to 1.5 magnitudes of visual extinction (*A_v*) that is located at a distance *d* = 700^{+1,500}_{−240} pc from the Sun. (ref. 12). The data cover the wavelength range 905–1,185 Å with a spectral resolution of about 20 km s^{−1}. FUSE^{13,14} is particularly well suited for studies of interstellar N₂, because all electronic ground-state transitions are only observable below 1,000 Å. The instrument generally provides two independent spectra for each wavelength region, which can be cross-checked. For the present study, we focus on the two silicon carbide (SiC) detectors covering wavelengths below 1,000 Å.

The data were reduced and calibrated with version 2.4.1 of the CalFUSE pipeline (ref. 15), which incorporates the appropriate Doppler corrections to remove the effects of spacecraft motion and place the data on the heliocentric velocity scale. Owing to the lack of onboard wavelength calibration, a zero-point uncertainty remains in the dispersion solution. To minimize uncertainties (±6 km s^{−1} per pixel; ref. 16) caused by the relative wavelength calibration, we used a cross-correlation technique to combine the individual exposures. To fix the absolute heliocentric velocity scale (*V*_{helioc}), we used interstellar H₂ lines in the FUSE data and archival CO data from the Space Telescope Imaging Spectrograph (STIS) on board the Hubble Space Telescope (HST), assuming CO and H₂ to be coexistent¹⁷. The final summed SiC 1B (SiC 2A) spectrum has a signal-to-noise ratio of 45 (50) per 9-pixel-resolution element at 958 Å.

Figure 1 shows the normalized 957–961 Å portion of the FUSE spectrum of HD 124314. Several strong absorption lines due to interstellar molecular hydrogen (H₂), deuterated molecular hydrogen (HD), and N I (refs 18–20) are clearly detected superposed on the broad stellar continuum, revealing at least two, barely resolved,

interstellar velocity components. In addition, there are weaker absorption features found in both SiC detector segments at the expected location of the 0–0 band of the c'₄¹Σ_u⁺ − X¹Σ_g⁺ transition of N₂ at 958.6 Å with a band oscillator strength (*f*_{band}) of 0.145 (ref. 21). These features are much too narrow to be stellar in nature because the star has a rotational velocity of 300 km s^{−1} (ref. 22). Examination of other, less reddened O6 stars, see Supplementary Fig. 1, reveal no evidence for photospheric absorption at this wavelength. No detector defects are present in either detector and other than N₂, no interstellar species have identified features at this wavelength.

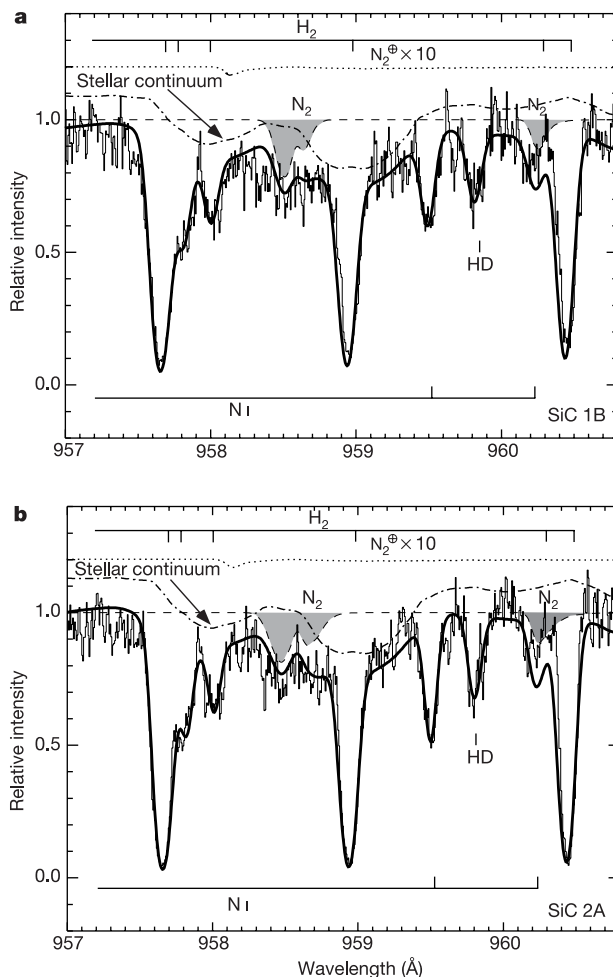


Figure 1 The N₂ portion of the normalized FUSE spectra of HD 124314. **a**, The SiC 1B data and **b**, the SiC 2A data (thin histograms). The thick solid line is the best fit of the data for the wavelength range 951–968 Å. Note that only the range from 957–961 Å is displayed here. All obvious interstellar absorption features (for example, H₂, N I, and so on) in this region are marked. The dot-dashed line is a stellar continuum model²³ with estimated stellar parameters of *T*_{eff} = 37,500 K and log(*g*) = 3.5. The stellar He II line at 959 Å line changes dramatically with the stellar parameters—and this directly affects the longer-wavelength N₂ trough at 958 Å. Inclusion of the c₃ N₂ band at 960 Å is vital in constraining the N₂ abundance. Therefore, the choice of stellar model does not change our detection of interstellar N₂. Before being incorporated into the profile-fitting program, the stellar model was rotationally broadened to 300 km s^{−1} (ref. 22). The offset between the data and the stellar model is caused solely by the line wing opacity (*τ*) of H₂. The best fit required two velocity components separated by 14 km s^{−1} for H₂, HD and N I, and similar results are obtained when using the O I velocity separation. Unrealistic parameter values resulted for a two-component fit to N₂. However, limiting the fit to one component in N₂, at the higher velocity, produced convergent fits. The dashed line filled with shading represents the normalized N₂ absorption profiles (*e*^{−τ}). Our detection of interstellar N₂ is not contaminated by telluric N₂ (dotted line), which has been scaled by a factor of ten and shifted up to 1.2 for the sake of clarity.

Many of the other N₂ bands are undetected owing to severe blending with more abundant species (for example, HI and H₂). For completeness, we have included the 0–0 band of the c₃¹Σ_u⁺ – X¹Σ_g⁺ transition of N₂ at 960.3 Å (*f*_{band} = 0.056) in our study because individual oscillator strengths (*f*-values) are available (G. Stark, personal communication), and although this band is blended with absorption from NI at 960.201 Å and H₂P(5) at 960.271 Å, the blending is not as severe as for the other stronger N₂ bands. Additionally, there are two N₂ bands outside the fitted wavelength range that are relatively unblended, but are so weak (*f*_{band} ≈ 0.02) that they are not detectable.

The N₂ absorption spectrum of the c₄' and c₃ transitions consists of many rotational lines²¹ under interstellar conditions. Our profile synthesis code⁷ explicitly treats the N₂ excitation and uses the laboratory wavelengths and *f*-values²¹ for the individual rotational lines, thereby reproducing the true N₂ line profiles. To evaluate whether the observed spectral features are due to interstellar N₂, we independently compared the 958 Å region of the SiC 1B and SiC 2A data to a synthetic spectrum combining a stellar model²³ and interstellar medium absorption from H₂ (*J* = 0–5), HD, NI, and N₂. The total synthetic spectrum was convolved to the FUSE resolution and then fitted to the data using a χ² minimization technique. No attempt was made to fit the weak CO band at 956 Å (ref. 24) because it does not significantly affect our fit. The profile synthesis parameters—temperature (*T*), Doppler broadening parameter (*b*-value) and column density (*N*)—were adjusted until a minimum χ² was obtained. Our best fits are shown overlying the data in Fig. 1 and the results are listed in Table 1. The apparent slight mismatch of some features in Fig. 1 (for example, the NI line at 960.2 Å) arise because the fit is based on a larger spectral region (951–968 Å) than is shown. Two velocity components are required to fit the interstellar H₂, HD, and NI, whereas only one component is required for N₂. It is important to note that because of the low instrumental resolution, we cannot reliably constrain the *b*-value for N₂. For numerical stability, the *b*-values of all species in the fit were constrained to coincide. Given that N₂ is likely to be restricted to the densest gas along the line of sight, its *b*-value might be smaller than that found for the other species. Therefore, our derived N₂ column must be treated as a lower limit.

Another consideration that needs to be addressed is the presence, if any, of telluric N₂ absorption. FUSE observations are designed to stop science exposures when the limb angle (θ_L) reaches 15°. There are a small number of exposures in the FUSE archives that extend below this, but the data quality is too low to place useful limits on the contribution expected from terrestrial N₂. The Hopkins Ultraviolet Telescope detected telluric N₂ absorption towards only those observations that went below θ_L < 15° (P. Feldman, personal communication). All our observations were taken with θ_L > 20°, so we calculated the expected contribution of telluric N₂ (that is, *N*(N₂)_{telluric}) using the National Space Science Data Center MSIS

model of the Earth's atmosphere²⁵ for the date of our observation, the satellite's altitude of 750 km, and θ_L = 20°. At this altitude, the space density of telluric N₂ is 2,200 cm⁻³ with a characteristic temperature of 1,100 K. We find *N*(N₂)_{telluric} = 1.1 × 10¹² cm⁻² for θ_L = 20°. As shown in Fig. 1, telluric N₂ with these characteristics does not significantly contribute to the observed spectrum.

To further assess our N₂ detection, we used ultra-high-resolution archival O I, S I, and CO STIS/HST data. HST observed HD 124314 on 10 April 1999 at a velocity resolution of 1.5 km s⁻¹. The normalized spectra are shown in Fig. 2. Because CO is a tracer of gas shielded from dissociating ultraviolet radiation^{17,26,27}, the facts that

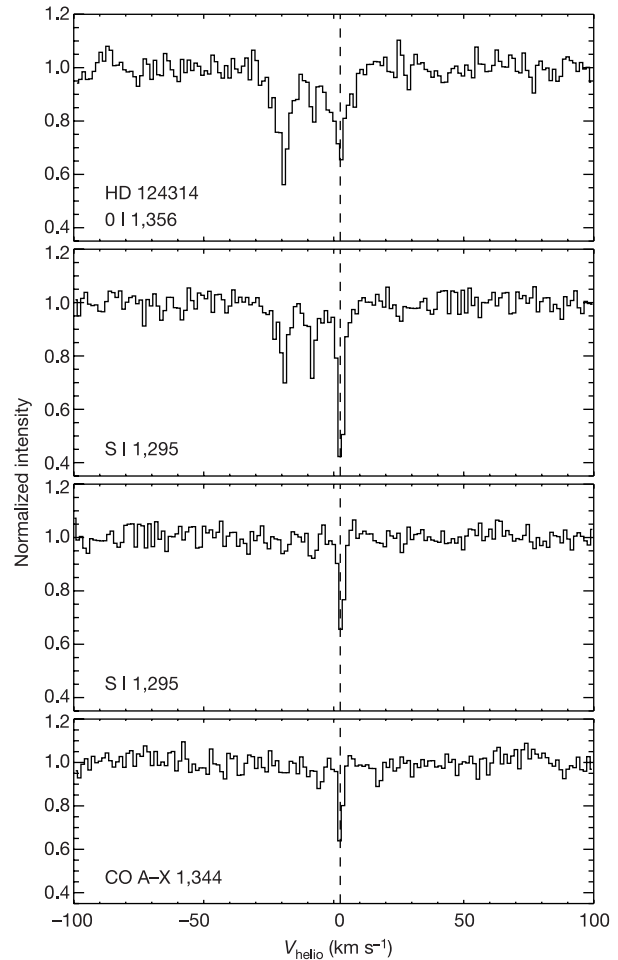


Figure 2 The normalized archival STIS/HST spectra of O I, S I and CO. This data reveals at least three velocity components in Interstellar O I line at 1,356 Å (two are dominant) and S I line at 1,295 Å, but only one component in Interstellar S I line at 1,296 Å and CO bands at 1,344 Å, 1,322 Å and 1,301 Å. These data indicate that the CO component is the densest interstellar cloud along the line of sight. Using a curve-of-growth analysis, the measured CO column density is well determined as: *M*(CO) = (7.6 ± 1.1) × 10¹³ cm⁻². We cannot accurately derive the *b*-value from these optically thin lines. We find that the S I doublet is slightly saturated. A curve of growth calculated for these two data points yields a S I column density of *M*(S I) = (1.6 ± 0.2) × 10¹³ cm⁻² and a *b*-value of 1.0 ± 0.1 km s⁻¹ for the longer-wavelength component. The velocity separation of 22 km s⁻¹ between the two dominant O I components is similar (within the uncertainties of the FUSE data) to the velocity separation of 14 km s⁻¹ we find from our analysis of H₂. The dashed line at ~3 km s⁻¹ represents the velocity to which the longer-wavelength H₂ component was normalized. The agreement in velocity separation between the two measured H₂ components and the two strongest O I components provides strong support for the adopted velocity structure used in our model. The fact that both N₂ and CO are found in the single densest component provides further support for the first detection of interstellar N₂.

Table 1 Results from profile synthesis

Species	<i>N</i> _{SiC 2A}	Literature values ^{7,10}
<i>N</i> (H ₂) (component 1)	(1.5 ± 0.2) × 10 ²⁰ cm ⁻²	...
<i>N</i> (H ₂) (component 2)	(1.4 ± 0.2) × 10 ²⁰ cm ⁻²	(3.3 ± 0.4) × 10 ²⁰ cm ⁻²
<i>T</i> ₁₋₀ (component 1)	340 ± 100 K	...
<i>T</i> ₁₋₀ (component 2)	38 ± 3 K	54 K
<i>N</i> (NI) (component 1)	(8.5 ± 1.0) × 10 ¹⁵ cm ⁻²	...
<i>N</i> (NI) (component 2)	(1.9 ± 0.3) × 10 ¹⁷ cm ⁻²	(2.21 ± 0.27) × 10 ¹⁷ cm ⁻²
<i>N</i> (N ₂) (component 2)	(4.6 ± 0.8) × 10 ¹³ cm ^{-2*}	...
<i>T</i> _{N₂} (component 2)	36 ± 5 K	...
<i>V</i> _{helioc} (component 1)	3.0 ± 0.5 km s ^{-1†}	...
<i>V</i> _{helioc} (component 2)	-17.0 ± 0.5 km s ⁻¹	...
<i>b</i> -value (component 1)	6.0 ± 0.5 km s ⁻¹	...
<i>b</i> -value (component 2)	7.0 ± 0.5 km s ⁻¹	...
Reduced χ ²	2.47	...

Results for SiC 1B agree within their mutual uncertainties to those for SiC 2A reported here.

* Average of SiC 1B and SiC 2A results.

† Set to coincide with the STIS/HST heliocentric velocity scale.

N₂ and CO both occur in the same velocity component, that the velocity separation in O I and H₂ agree, and that the CO component is aligned in velocity with the higher-velocity O I component strongly supports our claim of the first detection of interstellar N₂. Our N₂ detection is further supported by the fact that the excitation temperatures of H₂ (1–0) and of N₂ agree for the longer-wavelength component. Although the N₂ *b*-value is not reliably determined, we use the SI *b*-value to improve our estimate and find $N(N_2) = (4.6 \pm 0.8) \times 10^{13} \text{ cm}^{-2}$. We note that SI may be more extended than CO or N₂ in interstellar space. Because nitrogen has a lower cosmic abundance compared to either carbon or oxygen, we believe that $N(N_2)$ should not be larger than $N(\text{CO})$ and should the true N₂ *b*-value be much smaller than that for SI (although this is unlikely), significant amounts of N₂ (that is, $N(N_2) > 10^{14} \text{ cm}^{-2}$) could be present. Our firm lower limit to $N(N_2)$ is not sensitive to the *b*-value or the choice of stellar model used to represent the stellar continuum. Taken together, these data strongly indicate that N₂ has been detected for the first time in the interstellar medium and with a column density of $N(N_2) > 3.8 \times 10^{13} \text{ cm}^{-2}$.

From our analysis of the O I line at 1,356 Å, we find $N(\text{O I}) = (6.77 \pm 0.50) \times 10^{17} \text{ cm}^{-2}$ for the component near 3 km s⁻¹. Using the observed $N(\text{O I})/N(\text{H}_{\text{tot}})$ ratio $(4.74 \pm 0.81) \times 10^{-4}$ (ref. 11), this component contains $N(\text{H}_{\text{tot}}) = 1.5 \times 10^{21} \text{ cm}^{-2}$, where $N(\text{H}_{\text{tot}}) = N(\text{H I}) + 2N(\text{H}_2)$. The amount of interstellar reddening for this component can be determined from the dust-to-gas ratio²⁸, which yields $E(B-V) = 0.26 \text{ mag}^{-1}$. Assuming that the ratio of total to selective extinction is 3.1 (ref. 29), we find that the total visual extinction is 0.8 mag. When we compare our results to models of interstellar gas-phase chemistry¹, none of the standard cloud models explain our observations. The observed N₂ fractional abundance is more than two orders of magnitude too low for dense cloud models and approximately two orders of magnitude larger than expected from models of diffuse clouds. The fact that N I shows a deficiency in its relative abundance for lines of sight with $N(\text{H}_{\text{tot}}) > 10^{21} \text{ cm}^{-2}$ would argue that dense cloud chemistry should be important for interstellar nitrogen. However, the measured N₂ abundance and upper limits for other sightlines⁷ do not account for the observed variations. Additionally, we find that the fractional abundance of N₂ towards HD 124314 is $N_2/\text{H}_2 = 3.3 \times 10^{-7}$, similar to those estimated from N₂H⁺ observations⁴ of dark molecular clouds. Therefore, the far-ultraviolet lines of N₂ provide a unique probe of interstellar nitrogen chemistry in the transition region from diffuse to dense molecular gas. □

Received 16 February; accepted 30 April 2004; doi:10.1038/nature02614.

1. Viala, Y. P. Chemical equilibrium from diffuse to dense interstellar clouds. I Galactic molecular clouds. *Astron. Astrophys. (Suppl.)* **64**, 391–437 (1986).
2. Bergin, E. A., Langer, W. D. & Goldsmith, P. F. Gas-phase chemistry in dense interstellar clouds including grain surface molecular depletion and desorption. *Astrophys. J.* **441**, 222–243 (1995).
3. Womack, M., Ziruiys, L. M. & Wyckoff, S. A survey of N₂H⁺ in dense clouds: Implications for interstellar nitrogen and ion-molecule chemistry. *Astrophys. J.* **387**, 417–429 (1992).
4. Womack, M., Ziruiys, L. M. & Wyckoff, S. Estimates of N₂ abundances in dense molecular clouds. *Astrophys. J.* **393**, 188–192 (1992).
5. Lutz, B. L., Owen, T. & Snow, T. P. Jr A search with *Copernicus* for interstellar N₂ in diffuse clouds. *Astrophys. J.* **227**, 159–162 (1979).
6. Sandford, S. A., Bernstein, M. P., Allamandola, L. J., Goorvitch, D. & Teixeira, T. C. V. S. The abundances of solid N₂ and gaseous CO₂ in interstellar dense molecular clouds. *Astrophys. J.* **548**, 836–851 (2001).
7. Knauth, D. C., Andersson, B.-G., McCandless, S. R. & Moos, H. W. Potential variations in the interstellar N I abundance. *Astrophys. J.* **596**, L51–L54 (2003).
8. Le Petit, F., Roueff, E. & Herbst, E. H₃⁺ and other species in the diffuse cloud towards ζ Persei: A new detailed model. *Astron. Astrophys.* **417**, 993–1002 (2004).
9. Walborn, N. R. The space distribution of the O stars in the solar neighborhood. *Astron. J.* **78**, 1067–1073 (1973).
10. Cruz-Gonzalez, C., Recillas-Cruz, E., Costero, R., Peimbert, M. & Torres-Peimbert, S. A catalogue of galactic O stars. The ionization of the low density interstellar medium by runaway stars. *Rev. Mex. Astron. Astrofis.* **1**, 211–259 (1974).
11. André, M. K. *et al.* Oxygen gas-phase abundance revisited. *Astrophys. J.* **591**, 1000–1012 (2003).
12. Perryman, M. A. C. *et al.* The HIPPARCOS catalogue. *Astron. Astrophys.* **323**, L49–L52 (1997).
13. Moos, H. W. *et al.* Overview of the Far Ultraviolet Spectroscopic Explorer mission. *Astrophys. J.* **538**, L1–L6 (2000).
14. Sahnou, D. J. *et al.* On-orbit performance of the Far Ultraviolet Spectroscopic Explorer satellite. *Astrophys. J.* **538**, L7–L11 (2000).

15. Dixon, W. V. & Sahnou, D. J. CalFUSE v2.2: An improved data calibration pipeline for the Far Ultraviolet Spectroscopic Explorer (FUSE) in astronomical data analysis software and systems XII. (Spec. Iss.; eds Payne, H.E., Jedrzejewski, R.I. & Hook, R. N.) *ASP Conf. Ser.* **295**, (2003) 241–244.
16. Knauth, D. C., Howk, J. C., Sembach, K. R., Lauroesch, J. T. & Meyer, D. M. On the origin of the high-ionization intermediate velocity gas toward HD 14434. *Astrophys. J.* **592**, 964–974 (2003).
17. Federman, S. R., Glassgold, A. E., Jenkins, E. B. & Shaya, E. J. The abundance of CO in diffuse interstellar clouds. An ultraviolet survey. *Astrophys. J.* **242**, 545–559 (1980).
18. Abgrall, H. & Roueff, E. Wavelengths, oscillator strengths and transition probabilities of the H₂ molecule for Lyman and Werner systems. *Astron. Astrophys. (Suppl.)* **79**, 313–328 (1989).
19. Abgrall, H., Roueff, E. & Viala, Y. Vibration-rotation transition probabilities for the ground electronic X¹Σ⁺ state of HD. *Astron. Astrophys. (Suppl.)* **50**, 505–522 (1982).
20. Morton, D. C. Atomic data for resonance absorption lines. III. Wavelengths longward of the Lyman limit for the elements hydrogen to gallium. *Astrophys. J.* **149**, 205–238 (2003).
21. Stark, G. *et al.* Line oscillator strength measurements in the 0–0 band of the c₁¹Σ_g⁺ – X¹Σ_g⁺ transition of N₂. *Astrophys. J.* **531**, 321–328 (2000).
22. Conti, P. S. & Ebbets, D. Spectroscopic studies of O-type stars. VII. Rotational velocities *V*_{sin*i*} and evidence for macroturbulent motions. *Astrophys. J.* **213**, 438–447 (1977).
23. Lanz, T. & Hubeny, T. A grid of non-LTE line-blanketed model atmospheres of O-type stars. *Astrophys. J. (Suppl.)* **146**, 417–441 (2003).
24. Sheffer, Y., Federman, S. R. & Andersson, B.-G. FUSE measurements of Rydberg bands of interstellar CO between 925 and 1150 Å. *Astrophys. J.* **597**, L29–L32 (2003).
25. Hedin, A. E. Extension of the MSIS thermospheric model into the middle and lower atmosphere. *J. Geophys. Res.* **96**, 1159–1172 (1991).
26. Clayton, R. N. Self shielding in the Solar Nebula. *Nature* **415**, 860–861 (2002).
27. Van Dishoeck, E. F. & Black, J. H. The photodissociation and chemistry of interstellar CO. *Astrophys. J.* **334**, 771–802 (1988).
28. Bohlin, R. C., Savage, B. D. & Drake, J. F. A survey of interstellar H I from L_α absorption measurements. II. *Astrophys. J.* **242**, 132–142 (1978).
29. Sneden, C., Gehrz, R. D., Hackwell, J. A., York, D. G. & Snow, T. P. Infrared colors and the diffuse interstellar bands. *Astrophys. J.* **223**, 168–179 (1978).

Supplementary Information accompanies the paper on www.nature.com/nature.

Acknowledgements We thank A. Fullerton, S. R. Federman, P. Feldman, E. B. Jenkins, P. Sonnentrucker and P. Wannier for discussions and G. Stark for sharing his unpublished N₂ *f*-values. This work is based on observations made with the NASA-CNES-CSA Far Ultraviolet Spectroscopic Explorer, which is operated for NASA by Johns Hopkins University.

Competing interests statement The authors declare that they have no competing financial interests.

Correspondence and requests for materials should be addressed to D.C.K. (dknauth@pha.jhu.edu).

A precision measurement of the mass of the top quark

DØ Collaboration*

*A list of authors and their affiliations appear at the end of the paper

The standard model of particle physics contains parameters—such as particle masses—whose origins are still unknown and which cannot be predicted, but whose values are constrained through their interactions. In particular, the masses of the top quark (M_t) and *W* boson (M_W)¹ constrain the mass of the long-hypothesized, but thus far not observed, Higgs boson. A precise measurement of M_t can therefore indicate where to look for the Higgs, and indeed whether the hypothesis of a standard model Higgs is consistent with experimental data. As top quarks are produced in pairs and decay in only about 10⁻²⁴ s into various final states, reconstructing their masses from their decay products is very challenging. Here we report a technique that extracts more information from each top-quark event and yields a greatly improved precision (of ± 5.3 GeV/*c*²) when compared to previous measurements². When our new result is combined with our published measurement in a complementary decay mode³ and with the only other measurements available², the new world average for M_t becomes⁴ 178.0 ± 4.3 GeV/*c*². As a